energies

MDPI

Article

Modified Activated Carbon as an Effective Hydrogen Adsorbent

Paweł Baran *, Bronisław Buczek and Katarzyna Zarębska

Faculty of Energy and Fuels, AGH University of Science and Technology, Al. Mickiewicza 30, 30-059 Cracow, Poland

* Correspondence: baranp@agh.edu.pl; Tel.: +48-12-617-20-79

Abstract: Hydrogen adsorption measurements were taken by the weighting method using the Sartorius low-pressure microbalance. Experiments were conducted at two temperatures: 77.5 and 300 K; the adsorbent used was active carbon obtained from wood and modified with potassium hydroxide. The porous structure of the carbon prior to and after modification was evaluated based on the nitrogen adsorption and desorption data. Thus, the densimetric characteristic of active carbon was modified; porous structures were developed in the range of micro-, meso- and macropores and the volume of hydrogen adsorbed at 77.5 K showed an almost four-fold increase. Modified active carbons are found to be suitable for applications in hydrogen storage systems.

Keywords: hydrogen; adsorption; storage; active carbon

Citation: Baran, P.; Buczek, B.; Zarębska, K. Modified Activated Carbon as an Effective Hydrogen Adsorbent. *Energies* **2022**, *15*, 6122. https://doi.org/10.3390/en15176122

Academic Editor: Mofazzal Hossain

Received: 13 July 2022
Accepted: 22 August 2022
Published: 23 August 2022

1. Introduction

Hydrogen has become one of the most important energy sources in the 21st century. In a long term, it may actually replace oil and petroleum. It is an ideal fuel because of its easy availability and for environmental reasons. The product of hydrogen burning is water vapour, which does not add to air pollution. Currently, hydrogen is mainly used in industrial applications, but it can also be used as a source of energy for the lighting and heating of buildings, for electricity generation and as an engine fuel. Fuel cells that utilise the reaction between hydrogen and oxygen are used to produce electricity; their first application was aerospace technology [1,2].

No matter the actual application, of particular importance is the hydrogen storage method. The simplest strategy involves the storage of compressed H_2. The main drawback, however, is the low density of H_2 in this phase. Storage of liquid H_2 does not have this disadvantage, although the hydrogen tank temperature needs to be maintained below the critical point for hydrogen (33.145 K). In the context of supplying power to the fuel cells, a most interesting option involves metal hydride storage using the reversed sorption, although a heavyweight hydrogen tank is required, and that still remains a major disadvantage. The density of stored hydrogen can be increased through the physical process of gas adsorption in porous adsorbents. The method relying on the adsorption processes seems promising, because hydrogen can be recovered from the adsorbent's surface at the room temperature without necessitating the use of the heating system to trigger gas desorption. There are studies exploring potential applications of such adsorbents as carbon nanotubes [3], graphene [4], carbon nanofibers [5], and active carbon [6–9]. Despite extensive research efforts made so far to obtain high-porosity carbon adsorbents with enhanced storage capacity, their practical applications for hydrogen storage are still limited.

In the gravimetric method the quantity of adsorbed gas is obtained directly from the increase in the adsorbent's weight, and measurements are taken using high-precision and high-sensitivity microbalances [10,11]. Jagiełło et al. investigated [12] gas adsorption under 0–6 MPa and at 119–319 K using a weight-type apparatus in which measurable weight was 4 µg. Cazorla-Amoros et al. [13] used the DMT Sartorius 4406 high-pressure sorption microbalance to investigate carbon dioxide adsorption on active carbon and obtained

adsorption isotherms at a pressure of up to 4 bars. The repeatability of measurement results was reported to be 1%. The same type of weight apparatus [14] was used in studies on adsorption of N_2, Ar and CH_4 with microporous adsorbents at a temperature of 258–418 K and under pressure of 0.1–20 MPa. The article [15] summarises the contents of previous research studies on hydrogen storage in porous materials, provides a thorough review of current work of its authors and outlines the directions for further research efforts.

This paper summarises the results of research work aimed at developing the porous structure of active carbons. With regards to storage projects, the adsorbent ought to contain micropores in the size range of approximately 1 nm. For that reason carbon was activated with KOH, which is a most effective method used to prompt the development of porous structure in carbon sorbents [16,17].

2. Materials and Methods

Testing was done on active carbon made from pinewood (Picazine) modified with potassium hydroxide (PicazineK) [18]. Picazine carbon was dried and then mixed with ground KOH in the ratio 1:3 (m/m). The treatment was carried out in a muffle furnace at a temperature of 1023 K in the atmosphere of neutral gas (N2). The mixture was rapidly heated up to 973 K, and then the temperature was raised to 1023 K at a rate of 10 K/min. Once this temperature was reached, the mixture was maintained at this temperature for 30 min and then cooled to ambient temperature. During the entire treatment process, the neutral gas (N_2) was flowing inside the furnace at a rate of 30 L/min. When the reaction mixture reached the ambient temperature, the potassium hydroxide present in the mixture was neutralized with 5% HCl solution. Thus, modified carbon produced a solution which remained green-colored during the initial period of rinsing. After each subsequent rinsing of the potassium base, the suspension was decanted and diluted with distilled water and its pH value was measured. This treatment was repeated several times, until the pH readout of the filtrate became 6.5. When the specified pH level was achieved, the active carbon was separated from the solution by filtration under reduced pressure of 10–15 mmHg, and the filter cake was rinsed with distilled water and dried at 393 K. The modified product was obtained with a yield of 60.5% (m/m). The KOH modified active carbon sample was denoted as Picazine K.

Active carbon is originally produced by chemical activation using orthophosphoric acid by Societe PICA, France [19]. Adsorption tests were also performed on 5.0 pure hydrogen supplied by Linde Gaz.

Bulk density of carbon was determined using the type PT-E Powder Characteristics Tester apparatus, its apparent density measurements were taken with the EDA GeoPyc 1360 system, and real density (helium density) was obtained using the Accu-Pyc 1330 pycnometer. Density measurement and calculation data are summarized in Table 1.

Table 1. Properties of the activated carbons used.

Properties	Picazine	Picazine K
Bulk density (n), g/cm^3	0.204	0.120
Apparent density (p), g/cm^3	0.450	0.325
Real density ((r), g/cm^3	1.777	2.669
Total porosity (εc), cm^3/cm^3	0.885	0.631
Volume of pores (V), cm^3/cm^3	1.660	2.702

The characteristics of the porous structure were determined basing on the low-temperature adsorption and desorption isotherms for nitrogen (77 K). High-precision sorption measurements were taken with the ASAP 2020 apparatus over a wide range of relative pressures, from approx. 10^{-7} down to 0.99. Prior to the measurements, carbon samples were vacuum heated at 423 K for 16 h. The obtained measurement data were used to determine key parameters of the porous structure of active carbon (Pic) and of carbon

modified with potassium hydroxide (PicK). The following porous structure parameters were calculated for the samples:

- Specific surface area according to Brunauer—Emmet—Teller (BET) methodology.
- Total pore volume for relative pressure $p/p_0 = 0.99$;
- Microporous structure parameters (pores with diameter up to 2 nm) according to Dubinin—Radushkevich, Dubinin—Astakhov and t-plot methods;
- Mesoporous structure parameters (pores with diameters of 2–50 nm)—volume and area distributions of mesopores according to Barrett-Joyner-Halenda (BJH) methodology;

The analysis was performed according to the recommendations of standards:

- ISO 9277:2010(E), Determination of the specific surface area of solids by gas adsorption—BET method;
- ISO 15901-2:2006(E), Pore size distribution and porosity of solid materials by mercury porosimetry and gas adsorption—Part 2: Analysis of mesopores and macropores by gas adsorption;
- ISO 15901-3:2007(E), Pore size distribution and porosity of solid materials by mercury porosimetry and gas adsorption—Part 3: Analysis of micropores by gas adsorption;
- NIST 2006, Porosity and Specific Surface Area Measurements for Solid Materials.

Measurement and calculation data are summarized in Table 2.

Table 2. Structural parameters of active carbons.

Parameter	Picazine	Picazine K
Specific surface area calculated using the BET method, S_{BET}, m^2/g	1462	2939
Total volume of pores for $p/p_0 = 0.99$, $V_{total}^{0.99}$, cm^3/g	1.024	1.488
Parameters of texture of micropores by Dubinin and Radushkevich (DR)		
Surface of micropores, S_{mikro}^{DR}, m^2/g	1392	2817
Volume of micropores, V_{mikro}^{DR}, cm^3/g	0.494	1.001
Adsorption energy in micropores, E_{mikro}^{DR}, kJ/mol	16.22	17.77
Parameters of texture of micropores by Dubinin and Astakhov (DA)		
Surface of micropores, S_{mikro}^{DA}, m^2/g	1127	2229
Volume of micropores, V_{mikro}^{DA}, cm^3/g	0.500	0.938
Adsorption energy in micropores, E_{mikro}^{DA}, kJ/mol	16.11	18.49
Mean diameter of pores, d_r, nm	1.78	1.68
Dominant diameter of pores, d_d, nm	1.60	1.54

Figures 1 and 2 presented the results of the DFT analysis.

A diagram of the apparatus used in hydrogen adsorption and desorption experiments is shown in Figure 3.

Adsorption and desorption isotherms were obtained using the low-pressure microbalance Sartorius [20,21]. A sample with a mass of approximately 0.1 g was used for the tests. The accuracy of the microbalance in the tested measurement range was 10 µg. The microbalance was placed in the air thermostat where the constant temperature of 300 K was maintained. The sample to be tested was placed on one pan and the counterweight was filled with a non-sorptive material. To remove adsorbed gases and vapors from the sample's surface, the system (with open valves V1 and V3) was degassed for 8 h using a vacuum pump to reach the static vacuum of 10^{-2} Pa, and to maintain a constant weight. Afterwards, the glass arms of the microbalance were immersed in vessels filled with liquid nitrogen. Subsequent points of the isotherm were determined using the pressure progression method by dosing gas to the system through valves V1 and V2. The adsorption equilibrium was obtained after about 15 min. Pressure control in the system was effected using a pressure

transducer P operating in the range of 0–1 bars. The desorption isotherm was obtained by gradually reducing the pressure in the system using the vacuum pump, via valves V1 and V3. The waiting time to determine the desorption equilibrium was approx. 30 min. Measurements of adsorption and desorption isotherms were carried out at 77.5 K and 300 K for both carbon samples. The results are summarized in Figures 4–7.

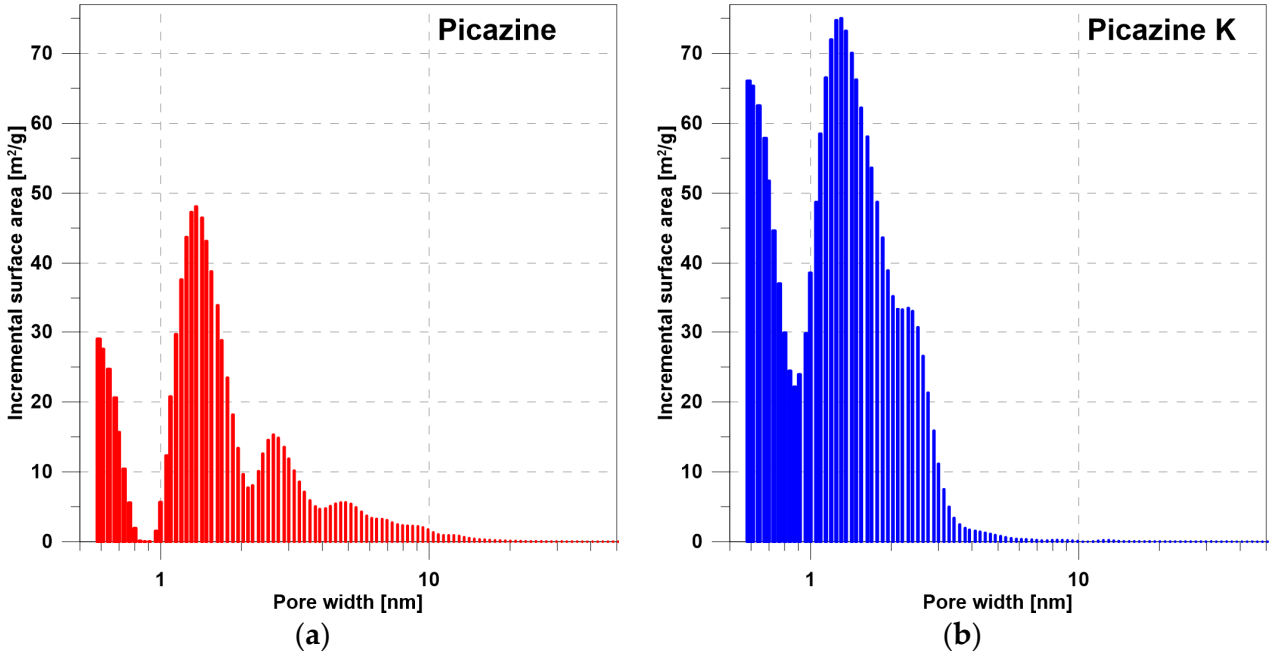

Figure 1. The dependence of the pore surface on the pore diameter determined by the DFT method for the (**a**) Picazine and (**b**) Picazine K samples.

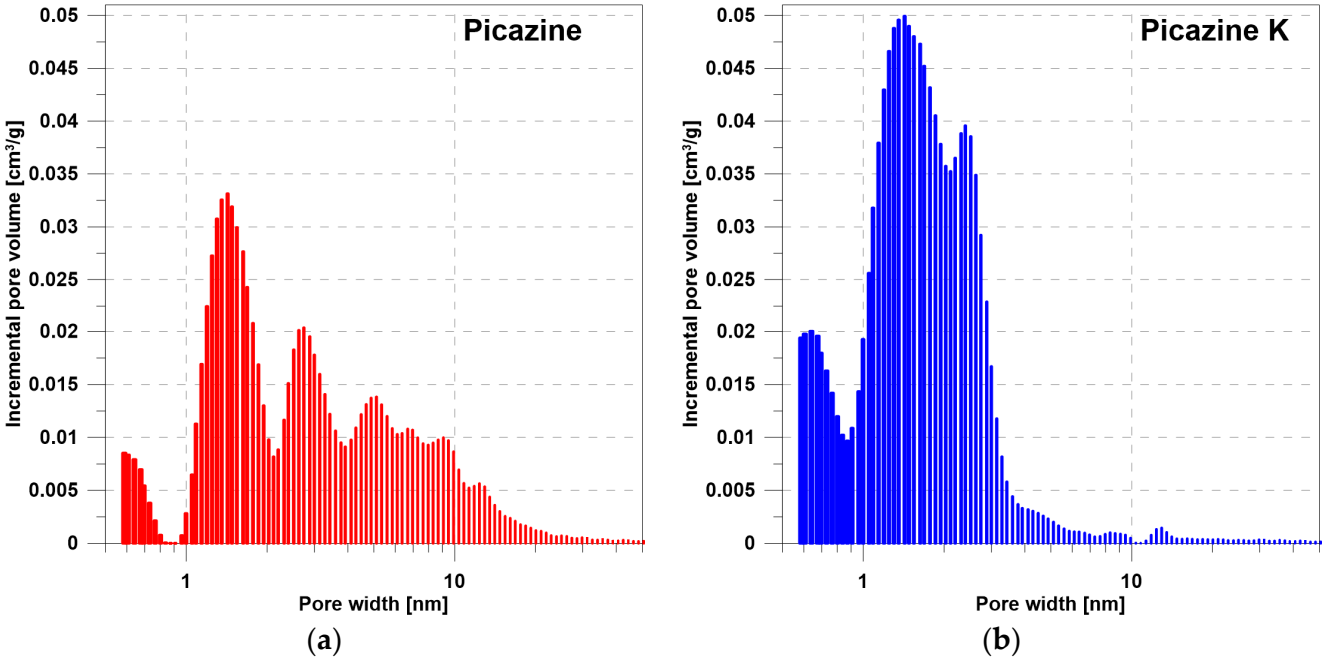

Figure 2. The dependence of the pore volume on the pore diameter determined by the DFT method for the (**a**) Picazine and (**b**) Picazine K samples.

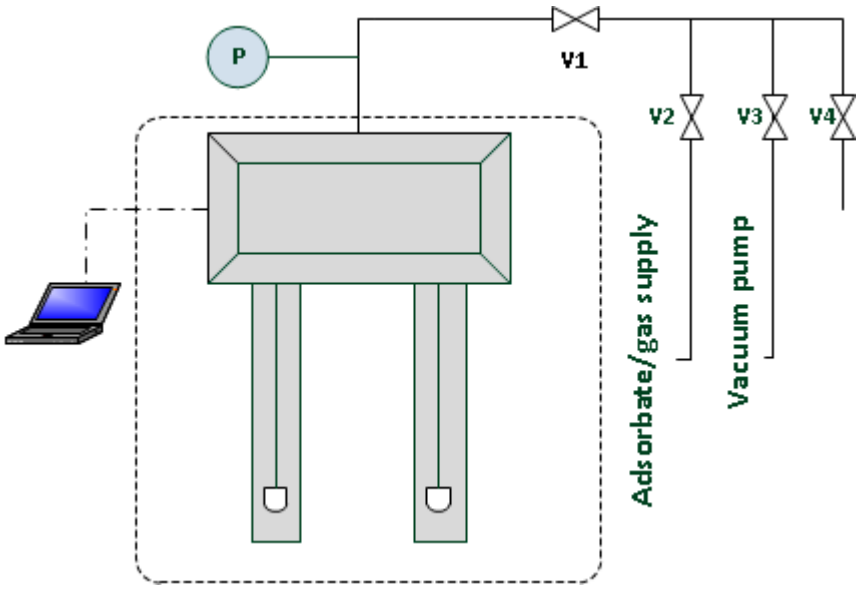

Figure 3. Apparatus used for measurements of hydrogen adsorption-desorption (V1-V4-valves, P-pressure transducer).

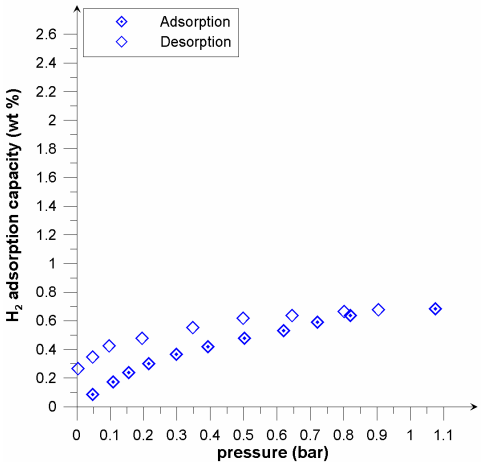

Figure 4. Adsorption/desorption isotherms of hydrogen onto Picazine at 77 K.

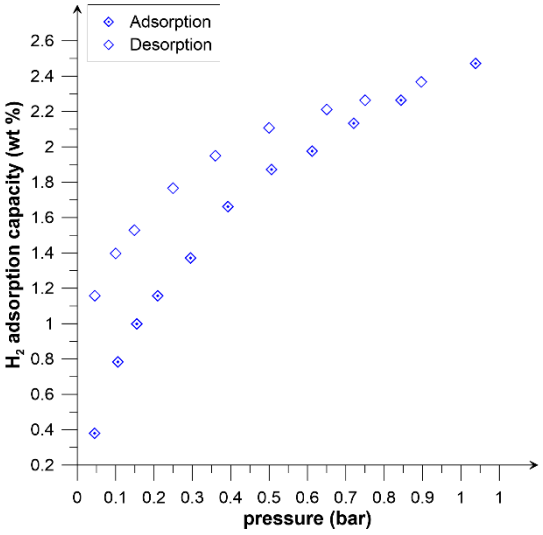

Figure 5. Adsorption/desorption isotherms of hydrogen on Picazine K at 77 K.

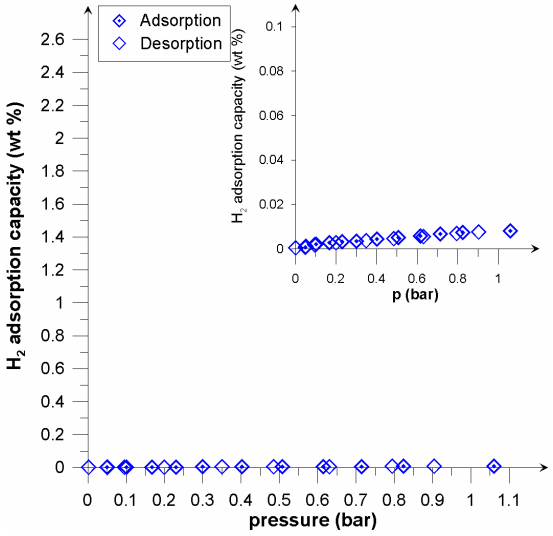

Figure 6. Adsorption/desorption isotherms of hydrogen on Picazine at 300 K.

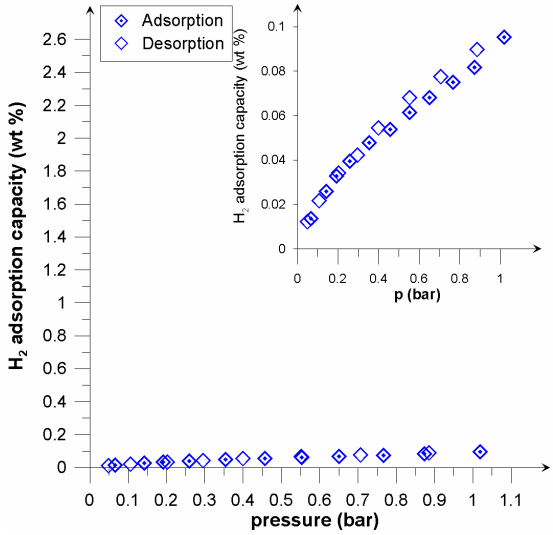

Figure 7. Adsorption/desorption isotherms of hydrogen on Picazine K at 300 K.

3. Results and Discussion

Based on the DFT analysis (Figures 1 and 2), it can be seen that the Picazine sample (before modification) was characterized by a dominant share of micropores, with a certain range of mesopores. Chemical activation of KOH changes the pore structure in the adsorbent. The presence of pores in the meso range disappears, while the share of micropores and submicropores increases significantly. This correlates with the pore volume values shown in Tables 2 and 3. In Table 2, the given volume values were calculated based on real and apparent densities. Table 3 shows the results of the analysis of adsorption isotherms which were fitted by the DR and DA equations. Both equations are applicable to describe adsorption isotherms on microporous materials. The calculated pore volume values presented in the manuscript are different, but this is due to the way they are calculated and the limitations of the models. Analyzing the results of the DFT analysis, we see that the range of pores includes both the range of micropores (in dominant quantity) and the range of narrower mesopores. Therefore, the values of constants calculated from the DR and DA equations may be subject to some uncertainty. Regardless, we see that there have been changes in these values after activation of the carbon material. In all cases, an increase is observed, a phenomenon which is also observed on hydrogen adsorption isotherms.

The analysis of measured hydrogen adsorption/desorption isotherms obtained at the temperature of liquid nitrogen reveals that the hydrogen adsorption capacity of the PicazineK carbon was nearly three times higher than that of the unmodified sample.

In both cases a hysteresis loop was registered. The potential occurrence of the capillary condensation phenomenon could be excluded due to the low critical temperature of hydrogen. The reported loop can be attributable to certain kinetic restrictions during the process of desorption.

The presence of a hysteresis loop has been previously registered in tests on other adsorbents. In the case of zeolites [22,23], it is reasonable to assume the occurrence of sealed micropores from which hydrogen cannot be removed. As regards nanotubes, the occurrence of a well- pronounced hysteresis loop in the H_2 adsorption/desorption isotherms measured at 77.5 K is consistent with a high energy barrier for desorption of H_2 molecules due to the presence of nanotubes with submicroporous inside-tube characteristics [24]. In the case of porous metal organic frameworks, it has been established that desorption restrictions are stronger at lower temperatures [25], and that they are also a function of the micropore radius [26]. Consequently, when pores are very narrow, they require higher temperature for desorption.

In the case of the investigated active carbons, the registered effects were similar to MOFs in relation to the nature of the microporous material. Calculations of the dominant pore diameters revealed a significant proportion of sub-micropores (Table 2). Recalling the McEnaney equation [27] for micropore size calculations, it was established that for the adsorption energy E_0 = 16.22, the micropore size becomes 0.40 nm, whilst for E_0 = 17.77, the size equals 0.36 nm in the slit pore model. An adsorbent having a high proportion of pores in this size will be a most promising material to be used in hydrogen storage systems [28,29]. Accordingly, the presence of hydrogen in the carbon structure was found to be molecular in nature. Similar values of sorption capacity at 77.5 K (excess hydrogen uptake) were obtained by Geng et al. [30]. Adsorption/desorption isotherms obtained at the ambient temperature are shown in Figures 6 and 7. In the case of the unmodified Picazine carbon, the adsorption capacity was found to be low (comparable to the measurement error). The modified PicazineK carbon had an adsorption capacity of 0.1 wt% (which corresponds to 12 cm^3 STP/g) (Figure 7). At room temperature, low- pressure sorption and desorption processes were found to be reversible, and in the context of practical applications this adsorbent does not seem appropriate for hydrogen storage. However, when comparing the results obtained for similar carbon adsorbents, including KOH activated ones, it is reasonable to suppose that in the elevated pressure range the properties of investigated samples might be more favorable in the context of potential applications. In their work, Minoda et al. [31] studied hydrogen sorption on active carbons, with rice hulls or PAN (Poly-acrylonitrile) as precursors. The specific surface and pore density of the samples thus obtained were similar to those of the carbon samples investigated in this study. One has to bear in mind, however, that experiments were conducted at elevated pressures. For the sample having the surface area 1600 m^2/g under the pressure 10 MPa the hydrogen uptake was 0.5%. Similarly, the hydrogen storage capacity of the sample S_{BET} 3000 m^2/g was found to be 0.7%.

According to the results of Panel et al. [32] and their literature analysis, the density of the adsorption monolayer is less than that of liquid hydrogen. This is directly due to the surface area of the hydrogen molecule that settles on the adsorbent, and it is also closely related to the distances between hydrogen molecules in the adsorption layer. This corresponds to Chahine's Rule which states that, in general, for every 500 m^2/g of surface area there is 1 wt% of hydrogen adsorption. Note, however, that the rule indicates the potential value of stored hydrogen relative to the specific surface area. The results obtained, show that KOH activation allowed the storage of about 2.5% of H^2 already at a pressure of 1 bar. This already relatively high adsorption value is related to the high proportion of micropores. Theoretical calculations [33,34] as well as experimental results [35] show that significant adsorption occurs in pores below 1.3 nm. These reports confirm a significant

increase in hydrogen adsorption on the PicazineK sample, resulting from an increase in the division of micropores formed by activation with KOH (Figure 1b).

Table 3. Hydrogen storage in various conditions using activated carbons.

Type of Adsorbent	S_{BET} (m^2/g)	H_2 Uptake (wt. %)	Storage Conditions	Additional Information	Ref.
AC from coffee beans	2070 2070	0.6 0.4	120 bar, 298 K 40 bar, 77 K	KOH activated	[36]
AC from anthracite	1149 2029 2849 3220 1308 2451 3073	3.2 4.9 6.0 5.7 2.9 5.8 5.7	40 bar, 77 K	KOH/NaOH activated	[37]
AC from pine	1055 1409	1.61 1.93	1 bar, 77 K	CO_2 activated	[38]
AC from low rank coal	640	0.29	40 bar, 77 K	KOH activated	[39]
AC from oil palm shell	3503	6.7 2.86	40 bar, 77 K 1 bar; 77 K	KOH activated	[40]
Carbon monolith from lignite	973	1.28	60 bar, 293 K	CO_2 activated	[41]
AC from stone of cherry laurel	1624	2.9	1 bar, 77 K	KOH activated	[42]

Investigations carried out using active carbon (Table 3) have shown that adsorption in activated carbon can be more efficient than compressed gas, but only at low temperatures. Chemical modification of adsorbents using KOH is known, although its impact varies [43]. In work by Lendzion-Bieluń et al., [44] the influence of chemical activation on WG-12 activated carbon was analyzed. This AC is obtained as a result of steam activation of hard coal with low ash content. As a result of the activation process with KOH, the surface area has remained virtually unchanged. It was different in the case of activated carbon obtained from the KOH activation of finger citron residue [45]. The use of KOH caused a very large development of the surface to acquire an adsorbent value similar to that obtained in this work (PicazineK). It seems, therefore, that a carbon precursor plays an important role in the chemical activation process using KOH. In the case of a compact structure that occurs in the case of low-ash hard coal, only the chemical surface area will change, and the nature of the texture will remain unchanged.

4. Conclusions

Adsorption experiments have demonstrated a substantial increase in adsorptive capacity of active carbon produced from pinewood on an industrial scale and then subjected to chemical activation with potassium hydroxide. It appears that the hydrogen adsorption capacity of the thus obtained active carbon is significantly higher than that of the unmodified sample at a temperature of 77.5 K. Key parameters of the porous structure of active carbon measured before and after the modification correlate well with the hydrogen adsorption rate determined by the gravimetric method.

In the context of those findings, the main consideration is whether the active carbon is a suitable material for practical applications, such as storage of gaseous fuels and distribution of gases which do not readily condense.

Author Contributions: Conceptualization, P.B. and B.B.; methodology, P.B. and B.B.; formal analysis, P.B., B.B. and K.Z.; investigation, P.B.; resources, P.B.; data curation, P.B., B.B. and K.Z.; writing—original draft preparation, P.B. and B.B.; writing—review and editing, P.B. and K.Z.; visualization, P.B.; supervision, P.B.; project administration, K.Z.; funding acquisition, K.Z. All authors have read and agreed to the published version of the manuscript.

Funding: This work was supported by the 'Initiative of Excellence—Research University—IDUB, Activity no. 8' programme of AGH UST in Krakow, Poland.

Conflicts of Interest: The authors declare no conflict of interest.

References

1. Broom, D.P. *Hydrogen Storage Materials: The Characterisation of Their Storage Properties*; Springer: London, UK, 2011; ISBN 9780857292216.
2. Sherif, S.A.; Goswami, D.Y.; Stefanakos, E.K.; Steinfeld, A. *Handbook of Hydrogen Energy*; CRC Press: Boca Raton, FL, USA, 2014; ISBN 9781420054477.
3. Singh, A.K.; Lu, J.; Aga, R.S.; Yakobson, B.I. Hydrogen Storage Capacity of Carbon-Foams: Grand Canonical Monte Carlo Simulations. *J. Phys. Chem. C* **2011**, *115*, 2476–2482. [CrossRef]
4. Darkrim Lamari, F.; Levesque, D. Hydrogen Adsorption on Functionalized Graphene. *Carbon N. Y.* **2011**, *49*, 5196–5200. [CrossRef]
5. Ryu, Z.; Rong, H.; Zheng, J.; Wang, M.; Zhang, B. Microstructure and Chemical Analysis of PAN-Based Activated Carbon Fibers Prepared by Different Activation Methods. *Carbon N. Y.* **2002**, *40*, 1144–1147. [CrossRef]
6. Texier-Mandoki, N.; Dentzer, J.; Piquero, T.; Saadallah, S.; David, P.; Vix-Guterl, C. Hydrogen Storage in Activated Carbon Materials: Role of the Nanoporous Texture. *Carbon N. Y.* **2004**, *42*, 2744–2747. [CrossRef]
7. Bhat, V.V.; Contescu, C.I.; Gallego, N.C.; Baker, F.S. Atypical Hydrogen Uptake on Chemically-Activated, Ultramicroporous Carbon. *Carbon N. Y.* **2010**, *48*, 1331–1340. [CrossRef]
8. Xiao, J.; Mei, A.; Tao, W.; Ma, S.; Bénard, P.; Chahine, R. Hydrogen Purification Performance Optimization of Vacuum Pressure Swing Adsorption on Different Activated Carbons. *Energies* **2021**, *14*, 2450. [CrossRef]
9. Ramirez-Vidal, P.; Canevesi, R.L.S.; Sdanghi, G.; Schaefer, S.; Maranzana, G.; Celzard, A.; Fierro, V. A Step Forward in Understanding the Hydrogen Adsorption and Compression on Activated Carbons. *ACS Appl. Mater. Interfaces* **2021**, *13*, 12562–12574. [CrossRef]
10. Ziemiański, P.P.; Derkowski, A.; Szczerba, M.; Guggenheim, S. Smectite Crystallite Swelling Under High Pressure of Methane. *J. Phys. Chem. C* **2021**, *125*, 7598–7610. [CrossRef]
11. Karbownik, M.; Dudzińska, A.; Strzymczok, J. Multi-Parameter Analysis of Gas Losses Occurring during the Determination of Methane-Bearing Capacity in Hard Coal Beds. *Energies* **2022**, *15*, 3239. [CrossRef]
12. Jagiełło, J.; Bandosz, T.J.; Schwarz, J.A. Application of Inverse Gas Chromatography at Infinite Dilution to Study the Effects of Oxidation of Activated Carbons. *Carbon N. Y.* **1992**, *30*, 63–69. [CrossRef]
13. Cazorla-Amorós, D.; Alcañiz-Monge, J.; Linares-Solano, A. Characterization of Activated Carbon Fibers by CO_2 Adsorption. *Langmuir* **1996**, *12*, 2820–2824. [CrossRef]
14. Salem, M.; Braeuer, P.; Szombathely, M. Thermodynamics of High-Pressure Adsorption of Argon, Nitrogen, and Methane on Microporous Adsorbents. *Langmuir* **1998**, *7463*, 3376–3389. [CrossRef]
15. Park, N.; Choi, K.; Hwang, J.; Kim, D.W.; Kim, D.O.; Ihm, J. Progress on First-Principles-Based Materials Design for Hydrogen Storage. *Proc. Natl. Acad. Sci. USA* **2012**, *109*, 19893–19899. [CrossRef] [PubMed]
16. Yoon, S.-H.; Lim, S.; Song, Y.; Ota, Y.; Qiao, W.; Tanaka, A.; Mochida, I. KOH Activation of Carbon Nanofibers. *Carbon N. Y.* **2004**, *42*, 1723–1729. [CrossRef]
17. Lillo-Ródenas, M.A.; Cazorla-Amorós, D.; Linares-Solano, A. Understanding Chemical Reactions between Carbons and NaOH and KOH: An Insight into the Chemical Activation Mechanism. *Carbon N. Y.* **2003**, *41*, 267–275. [CrossRef]
18. Buczek, B. Adsorption of Methane and Carbon Dioxide on a Potassium Hydroxide-Modified Activated Carbon. *Przem. Chem.* **2013**, *92*, 535–537.
19. Perrin, A.; Celzard, A.; Marêché, J.F.; Furdin, G. Improved Methane Storage Capacities by Sorption on Wet Active Carbons. *Carbon* **2004**, *42*, 1243–1249. [CrossRef]
20. Baran, P.; Cygankiewicz, J.; Zarębska, K. Carbon Dioxide Sorption on Polish Ortholignite Coal in Low and Elevated Pressure. *J. CO_2 Util.* **2013**, *3–4*, 44–48. [CrossRef]
21. Baran, P.; Krzak, M.; Zarebska, K.; Szczurowski, J.; Zmuda, W.A. Adsorption of Sulfur(IV) Oxide on Activated Carbon from Pyrolysis of Waste Tires. *Przem. Chem.* **2016**, *95*, 1164–1166. [CrossRef]
22. Fujiwara, M.; Fujio, Y.; Sakurai, H.; Senoh, H.; Kiyobayashi, T. Storage of Molecular Hydrogen into ZSM-5 Zeolite in the Ambient Atmosphere by the Sealing of the Micropore Outlet. *Chem. Eng. Process. Process Intensif.* **2014**, *79*, 1–6. [CrossRef]
23. Masika, E.; Mokaya, R. Preparation of Ultrahigh Surface Area Porous Carbons Templated Using Zeolite 13X for Enhanced Hydrogen Storage. *Prog. Nat. Sci. Mater. Int.* **2013**, *23*, 308–316. [CrossRef]
24. Czosnek, C.; Baran, P.; Grzywacz, P.; Baran, P.; Janik, J.F.; Rózycka, A.; Sitarz, M.; Jeleń, P. Generation of Carbon Nanostructures with Diverse Morphologies by the Catalytic Aerosol-Assisted Vapor-Phase Synthesis Method. *Comptes Rendus Chim.* **2015**, *18*, 1198–1204. [CrossRef]

25. Rowsell, J.L.C.; Yaghi, O.M. Effects of Functionalization, Catenation, and Variation of the Metal Oxide and Organic Linking Units on the Low-Pressure Hydrogen Adsorption Properties of Metal−Organic Frameworks. *J. Am. Chem. Soc.* **2006**, *128*, 1304–1315. [CrossRef] [PubMed]
26. Panella, B.; Hirscher, M.; Ludescher, B. Low-Temperature Thermal-Desorption Mass Spectroscopy Applied to Investigate the Hydrogen Adsorption on Porous Materials. *Microporous Mesoporous Mater.* **2007**, *103*, 230–234. [CrossRef]
27. McEnaney, B. Estimation of the Dimensions of Micropores in Active Carbons Using the Dubinin-Radushkevich Equation. *Carbon N. Y.* **1987**, *25*, 69–75. [CrossRef]
28. Wang, J.; Kaskel, S. KOH Activation of Carbon-Based Materials for Energy Storage. *J. Mater. Chem.* **2012**, *22*, 23710–23725. [CrossRef]
29. Wang, H.; Gao, Q.; Hu, J. High Hydrogen Storage Capacity of Porous Carbons Prepared by Using Activated Carbon. *J. Am. Chem. Soc.* **2009**, *131*, 7016–7022. [CrossRef]
30. Geng, Z.; Zhang, C.; Wang, D.; Zhou, X.; Cai, M. Pore Size Effects of Nanoporous Carbons with Ultra-High Surface Area on High-Pressure Hydrogen Storage. *J. Energy Chem.* **2015**, *24*, 1–8. [CrossRef]
31. Minoda, A.; Oshima, S.; Iki, H.; Akiba, E. Synthesis of KOH-Activated Porous Carbon Materials and Study of Hydrogen Adsorption. *J. Alloys Compd.* **2013**, *580*, S301–S304. [CrossRef]
32. Panella, B.; Hirscher, M.; Roth, S. Hydrogen Adsorption in Different Carbon Nanostructures. *Carbon N. Y.* **2005**, *43*, 2209–2214. [CrossRef]
33. Rzepka, M.; Lamp, P.; de la Casa-Lillo, M.A. Physisorption of Hydrogen on Microporous Carbon and Carbon Nanotubes. *J. Phys. Chem. B* **1998**, *102*, 10894–10898. [CrossRef]
34. Wang, Q.; Johnson, J.K. Molecular Simulation of Hydrogen Adsorption in Single-Walled Carbon Nanotubes and Idealized Carbon Slit Pores. *J. Chem. Phys.* **1998**, *110*, 577–586. [CrossRef]
35. Gogotsi, Y.; Portet, C.; Osswald, S.; Simmons, J.M.; Yildirim, T.; Laudisio, G.; Fischer, J.E. Importance of Pore Size in High-Pressure Hydrogen Storage by Porous Carbons. *Int. J. Hydrog. Energy* **2009**, *34*, 6314–6319. [CrossRef]
36. Akasaka, H.; Takahata, T.; Toda, I.; Ono, H.; Ohshio, S.; Himeno, S.; Kokubu, T.; Saitoh, H. Hydrogen Storage Ability of Porous Carbon Material Fabricated from Coffee Bean Wastes. *Int. J. Hydrog. Energy* **2011**, *36*, 580–585. [CrossRef]
37. Fierro, V.; Szczurek, A.; Zlotea, C.; Marêché, J.F.; Izquierdo, M.T.; Albiniak, A.; Latroche, M.; Furdin, G.; Celzard, A. Experimental Evidence of an Upper Limit for Hydrogen Storage at 77 K on Activated Carbons. *Carbon N. Y.* **2010**, *48*, 1902–1911. [CrossRef]
38. Rowlandson, J.L.; Coombs OBrien, J.; Edler, K.J.; Tian, M.; Ting, V.P. Application of Experimental Design to Hydrogen Storage: Optimisation of Lignin-Derived Carbons. *C J. Carbon Res.* **2019**, *5*, 82. [CrossRef]
39. Harjanto, S.; Noviana, L.N.; Diniati, M.; Yunior, S.W.; Nasruddin. Hydrogen Adsorption Capacity Reduction of Activated Carbon Produced from Indonesia Low Rank Coal by Pelletizing. *Sains Malays.* **2015**, *5*, 747–752. [CrossRef]
40. Zhao, W.; Luo, L.; Chen, T.; Li, Z.; Zhang, Z.; Fan, M. Activated Carbons from Oil Palm Shell for Hydrogen Storage. *IOP Conf. Ser. Mater. Sci. Eng.* **2018**, *368*, 12031. [CrossRef]
41. Alfadlil, B.R.; Knowles, G.P.; Parsa, M.R.; Subagyono, R.R.D.J.N.; Daniel; Chaffee, A.L. Carbon Monolith from Victorian Brown Coal for Hydrogen Storage. *J. Phys. Conf. Ser.* **2019**, *1277*, 12024. [CrossRef]
42. Toprak, A. Production and Characterization of Microporous Activated Carbon from Cherry Laurel (*Prunus laurocrasus* L.) Stone: Application of H_2 and CH_4 Adsorption. *Biomass Convers. Biorefinery* **2020**, *10*, 977–986. [CrossRef]
43. Williams, N.E.; Oba, O.A.; Aydinlik, N.P. Modification, Production, and Methods of KOH-Activated Carbon. *ChemBioEng Rev.* **2022**, *9*, 164–189. [CrossRef]
44. Lendzion-Bieluń, Z.; Czekajło, Ł.; Sibera, D.; Moszyński, D.; Sreńscek-Nazzal, J.; Morawski, A.W.; Wrobel, R.J.; Michalkiewicz, B.; Arabczyk, W.; Narkiewicz, U. Surface Characteristics of KOH-Treated Commercial Carbons Applied for CO_2 Adsorption. *Adsorpt. Sci. Technol.* **2017**, *36*, 478–492. [CrossRef]
45. Dai, W.; Liu, Y.; Su, W.; Hu, G.; Deng, G.; Hu, X. Preparation and CO_2 Sorption of a High Surface Area Activated Carbon Obtained from the KOH Activation of Finger Citron Residue. *Adsorpt. Sci. Technol.* **2012**, *30*, 183–191. [CrossRef]